KKU ENGINEERING JOURNAL 2016;43(S2):294-298 Research Article

KKU Engineering Journal

https://www.tci-thaijo.org/index.php/kkuenj/index

Maximum temperature prediction for concrete sections during cooling phase

Pattamad Panedpojaman* and Pong-in Intarit

Department of Civil Engineering, Faculty of Engineering, Prince of Songkla University, Thailand.

Received April 2016
Accepted June 2016

Abstract

Maximum temperatures at each location within a concrete cross section exposed to fire during both heating and cooling phases are required to evaluate residual strength of RC members. Available methods for predicting the maximum temperature have been limited to complicated numerical methods. Therefore, this study proposed a simplified equation to predict the maximum temperature by using a parametric study based on a validated finite element (FE) model. One dimensional heat transfer analysis under a standard fire curve was a scope of this study. Investigated parameters were section thicknesses, fire durations and cooling durations. Based on the parametric study and an energy based method, simplified equations to evaluate the maximum temperature during the cooling duration of 4 h were proposed. The equations were formulated as functions of an effective thickness, a temperature at the non-fire exposed surface and an exponent of temperature profiles at the end of the heating phase. Comparing with those of the FE results, the predicted maximum temperatures agree well and have the coefficient of determination of 0.9737.

Keywords: Concrete section, Cooling phase, Energy based method, Maximum temperature

1. Introduction

Since temperatures in reinforcing steel and concrete are increased under fire exposure, concrete members experience loss of strength and stiffness. The maximum temperatures at each location within a concrete cross section are required to evaluate residual strengths of concrete members [1-2]. Available methods for predicting the maximum temperature have been limited to complicated numerical methods [1-2]. For designing structures exposed to a natural fire, heating and cooling phases must be considered. Based on EN1991-1-2, the cooling duration is generally less than 4 h. Due to transferring of heat energy within the section, the maximum temperature is reached once fire duration has elapsed into the cooling phase.

Only a few simplified methods to predict temperatures in concrete sections are available in the heating phase [3-5]. The simplified methods [2-4] are useful and simple but provide an accurate temperature prediction only for thick sections. As an alternative simplified method, the energy based method (EBM) [5] provides more accurate temperature prediction for one dimensional (1D) heat transfer under the heating phase. However, the prediction in the cooling phase is limited. Therefore, this study aims to extend the temperature prediction of the EBM into the cooling phase. The standard fire curve of EN1991-1-2 is scoped in the study.

2. Energy based method

To extend the evaluation of the EBM, the method is briefly described. To simplify the one dimensional (1D) heat transfer analysis, the pre-determined temperature function within cross sections $T^n(x)$ were used as given in Eqs. (1-2) [5]. A uniform grid for each time was used in the method. As a convenient shorthand notation, T^n represents the temperature at time $t = n\Delta t$. n is the index for time.

$$T^n(x) = \left(T_s^n - T_0^n\right)\left(\left(b'^n - x\right)/b'^n\right)^{\alpha^n} + T_0^n \quad (1)$$

$$\alpha^n = -0.7\ln\left(\Delta T_0^{n-1}/T_s^{n-1}\right) + 1.4 \quad (2)$$

where T_s^n is the temperature at the fire exposed surface, T_0^n is the temperature at the effective depth b'^n or at the non-fire exposed surface, α^n is the exponent of the temperature function, x is the given concrete depth from the fire exposed surface, and ΔT_0^n is the temperature increment of T_0^n from the room temperature T_r. The temperature function and exponent were derived based on investigation of the temperature profiles observed from a finite element model (FEM) of various concrete sections. This pre-determined shape function is suitable for monotonically increasing fire curves, but not in the cooling phase.

To evaluate the surface temperature (T_s^n), partial differential equations of heat transfers were numerically solved based on the finite difference method (FDM) and the pre-determined temperature function as

*Corresponding author. Tel +66 7428 7140
Email address: ppattamad@eng.psu.ac.th
doi: 10.14456/kkuenj.2016.113

$$T_s^n = \frac{2\Delta t}{\rho c \Delta x}\left[q^n - k^n \alpha^n \frac{\left(T_s^{n-1} - T_0^{n-1}\right)}{b'^{n-1}}\right] + T_s^{n-1} \geq T_s^{n-1} \quad (3)$$

$$q^n = h\left(T_f^{n-1/2} - T_s^{n-1}\right) + \varepsilon\sigma\left(\left(T_f^{n-1/2}\right)^4 - \left(T_s^{n-1}\right)^4\right) \quad (4)$$

where ρ and c are the concrete density and specific heat, q^n is the surface heat flux, T_f is the fire temperature, h is the convection coefficient, ε and σ are the emissivity and Stefan Boltzmann constant for radiative heat transfer. Note that T_f is evaluated at the middle of a time step ($T_f^{n-1/2}$) as a representative fire temperature in that time step. Based on the conservation of energy transferred to a section from fire, b'^n and T_0^n can be computed as

$$b'^n = \frac{Q_T^n\left(\alpha^n + 1\right)}{\rho c\left(T_s^n - T_r\right)} \geq b'^{n-1} \quad (5)$$

$$T_0^n = \frac{1}{\alpha^n}\left[\left(\alpha^n + 1\right)\left(\frac{Q_T^n}{\rho c b} + T_r\right) - T_s^n\right] \geq T_r \text{ and } T_0^{n-1} \quad (6)$$

$$Q_T^n = \int_0^{t^n} qA dt \approx \sum_{m=0}^{n} A\left(q^n\right)\Delta t \quad (7)$$

Q_T^n is the amount of heat energy in that section, A is the area of the fire-exposed surface and b is the section thickness. Further details of the energy based method can be study in [5].

3. FE model

To conduct a parametric study of the maximum temperature profiles in concrete sections, finite element models (FEM) were simulated by using the ANSYS software. Concrete sections were simulated as three-dimensional model with unit length as shown in Figure 1(a). Solid element (Solid 70), and the surface element (Surf152) were used. Solid70 is a brick element having eight nodes with a single degree of freedom, i.e. the temperature. Solid70 is suitable for conductive heat transfer analysis. At the fire exposed surface, the surface element is applied to account for both convection and radiation of heat from fire. Based on a sensitivity study of the temperature–time curve, the time step size and the solid element size were selected as 60 seconds and *b/20*, respectively. *b* is the section thickness or width of FE models.

All thermal properties were specified as recommended in EN1991-1-2. However, h and ε were set as 20 W/m^{2}K and 0.3, respectively [6]. In the FEM, the non-fire exposed surfaces were considered as an adiabatic boundary condition. The FE model was validated against slab and beam experiments reported in the literature [7-8] as shown in Figures 2(a)-2(d). On an average, the temperature-time curves obtained from the FE model agree well with the experiments. Note that the real thermal properties in the experiment are unknown. The specified thermal properties may cause the deviations between the experiments and FE results.

In Figures 2(c) and 2(d), they clearly show that the maximum temperature of the measured location is reached in the cooling phase not the heating phase. The maximum temperature increases from the heating phase higher than 100 ^{o}C in the short fire duration as shown in Figure 2(d). Such increments significantly affect residual strength.

4. Parametric study and proposed temperature equations

Six thicknesses: 10, 15, 20, 25, 40 and 50 cm, four heating durations: 1, 2, and 4 h and five cooling durations: 0, 1, 2, 3, and 4 h were scoped in this parametric study through the validated FE model. Using a full factorial design for the computational experiments, there are 90 (6×3×5) data sets generated.

The FE results describe that, at the end of the heating phase, heat energy is high in concrete layers near the fire exposed surface but low in concrete layers far from the fire exposed surface. During the cooling phase, the higher heat energy transfers into the deeper layers having the lower heat energy and loses at the fire exposed surface. The heat transfer within the sections causes temperature increasing in the deeper layer, even in the cooling phase as shown in Figures 1(b) and 1(c). Based on temperature profiles variations with fire durations, the maximum temperature profile can be plotted as shown an example in Figure 1(c) for the 20-cm thick section. Since the heat loses at the fire exposed surface during the cooling phase, the maximum T_s^n occurs at the end heating duration. Increment of the maximum temperature is zero at the fire exposed surface but positive within the inner part.

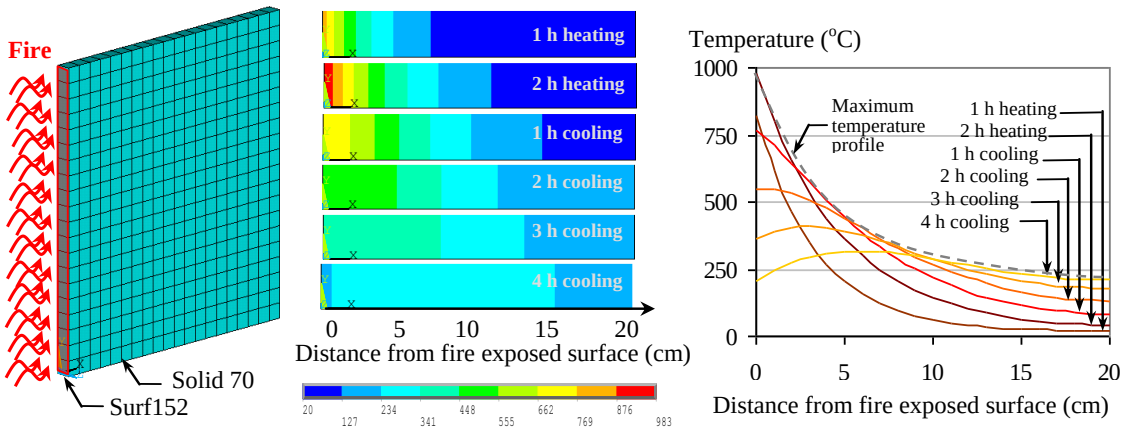

Figure 1 FE model and result: (a) FE model, (b) temperature contour along the thickness and (c) temperature profiles along the thickness

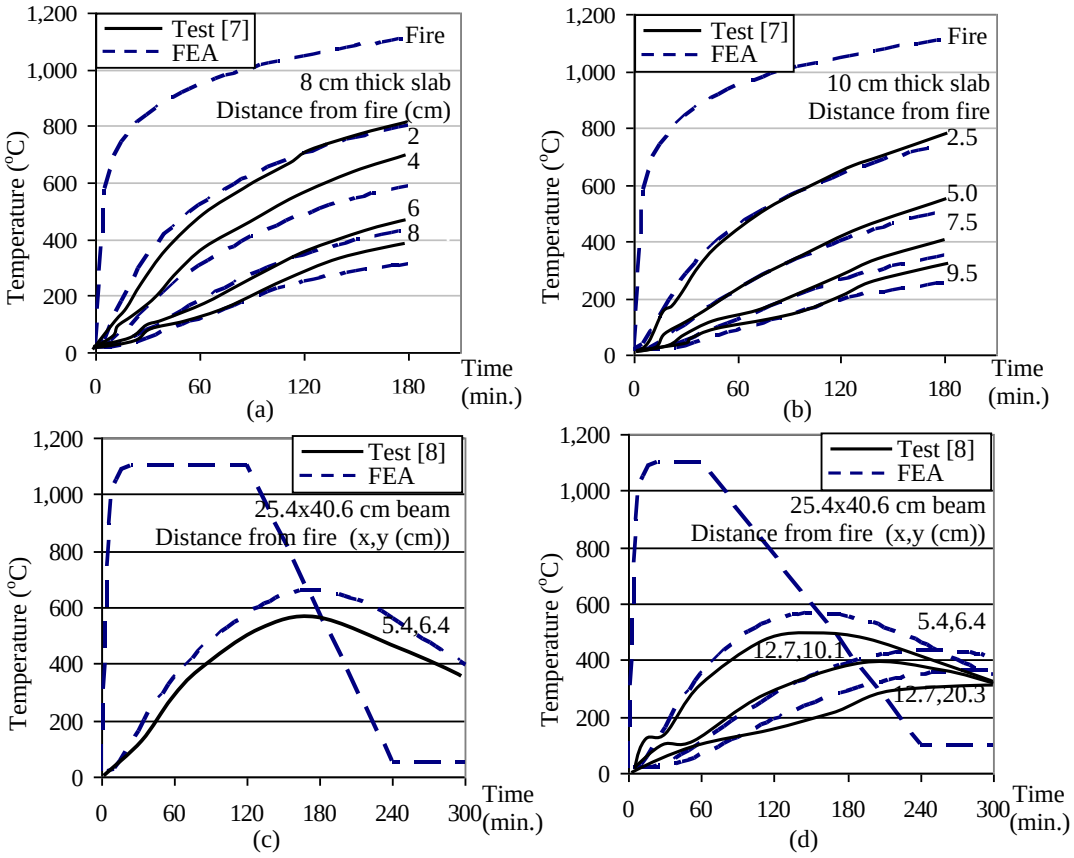

Figure 2 Comparison of temperature-time curves between the experiments and the FE models: (a) 8 cm thick slab, (b) 10 cm thick slab, (c) 25.4x40.6 cm beam under 2 h fire duration and (d) 25.4x40.6 cm beam under 1 h fire duration

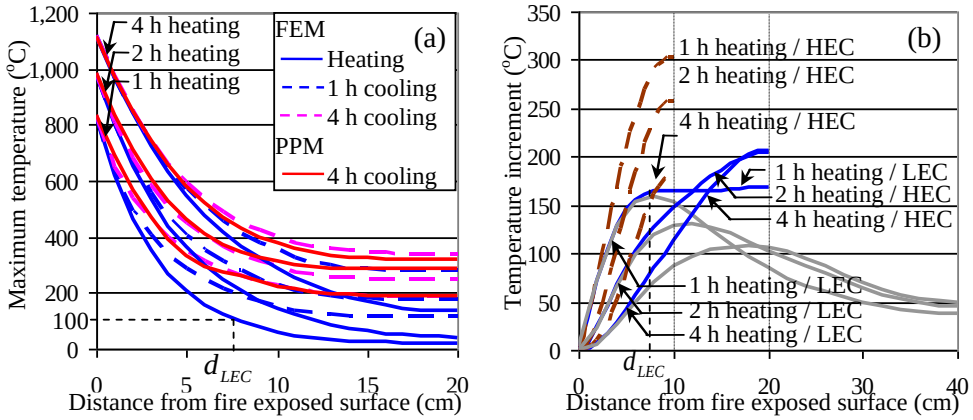

Figure 3 Variation of the temperature profiles along the concrete depth: (a) the maximum temperature and (b) the temperature increment

As an example of the FE results, the maximum temperature (T_{CL}^{n}) profiles of the 20-cm thick section and increments of the maximum temperature during the cooling phase (ΔT_{CL}^{n}) of the 10, 20 and 40-cm thick sections are shown in Figures 3(a) and 3(b), respectively. It can be observed in Figure 3(a) that longer cooling durations provides higher maximum temperature. For the longer cooling durations, the ambient temperature is slowly cooling. The energy loss at the surface is decelerated. As a result, the maximum temperature in the inner part is higher than those of the shorter cooling durations.

Based on the FE results, two energy cases are identified based on temperatures at the end of the heating phase: high energy case (HEC) and low energy case (LEC). For the HECs, temperatures at the non-fire exposed surface are significantly higher than the room temperature. On the other hand, temperatures at the non-fire exposed surface are low and close to the room temperature for the LECs. The HECs and LECs generally occur in thin sections or long fire durations and in thick sections or short fire durations, respectively.

For the HECs, the temperature increments (ΔT_{CL}^{n}) as shown in Figure 3(b) are monotonically higher with deeper depths. The temperature increment reaches its maximum at the non -fire-exposed surface. Even though, heat energy in the sections loses at the fire exposed surface, the energy in

concrete layers near the fire exposed surface is high enough to increase the temperature increment throughout the sections during the cooling phase. The temperature increment reaches its maximum at the non-fire exposed surface. Magnitude of the maximum increment ($\Delta T^n_{CL,max}$) depends on the section thickness (b) and magnitude of T^n_0 at the end heating duration. The overall maximum temperature profiles shows a flatter shape comparing with the profiles at the end of the heating phase. As a result, the profile exponent during cooling phase (α^n_{CL}) is generally higher than that of the heating phase (α^n).

For the LECs, ΔT^n_{CL} is higher with deeper depths and reaches its maximum ($\Delta T^n_{CL,max}$) at a certain depth and lower after that as shown in Figure 3(b). The heat energy in these sections is not enough to increase the temperature increment throughout the sections. $\Delta T^n_{CL,max}$ is found at about the depth (d_{LEC}) which having temperature of 100 °C at the end heating duration, that is $T^n(d_{LEC}) = 100$ °C. Magnitude of $\Delta T^n_{CL,max}$ tends to depend on d_{LEC}. Similarly to the HECs, the overall maximum temperature profiles are also flatter shape comparing with the profiles at the end heating duration. Therefore, overall α^n_{CL} is also higher α^n for the LECs. However, the increment curves as shown in Figure 3(b) are not monotonically increasing. The maximum temperature profiles must be separated into two parts: before and after d_{LEC}. Since high temperatures in the profile before d_{LEC} are significant for computations of residual strength, this study focuses on this part of the profile. It can be observed that the temperature increment causes the profile slope is steeper and α^n_{CL} is lower than α^n in this part.

Based on an empirical study, equations to predict T^n_{CL} after the cooling duration of 4 h are distinguished as the high and low energy cases and given in Eq. (8) and Table 1. Note that d_{LEC} and T^n_0 can be computed by the EBM. For the LECs, the temperature increment after d_{LEC} is assumed to be constant up to the non-fire exposed surface. As a result, $T^n_{CL}(x)$ for $x > d_{LEC}$ can be computed in Eq. (9).

$$T^n_{CL}(x) = \left(T^n_s - T^n_{0,CL}\right)\left((b_{CL} - x)/b_{CL}\right)^{\alpha^n_{CL}} + T^n_{0,CL} \quad \text{for } x < b_{CL} \tag{8}$$

$$T^n_{CL}(x) = T^n(x) + \Delta T^n_{CL,\max} \quad \text{for } x > d_{LEC} \tag{9}$$

An example of the proposed T^n_{CL} profiles is also shown in Figure 3(a). The overall comparisons of the proposed ΔT^n_{CL} and T^n_{CL} with the FEM results at a nodal point of *b/20* along the section thickness of all investigated cases are depicted in Figure 4. The predicted temperatures agree well with the FEM results with slight deviations. The coefficient of determinations from the comparison of ΔT^n_{CL} and ΔT^n_{CL} are 0.7818 and 0.9737, respectively. Note that the significantly conservative errors up to 120 °C in Figure 4(a) are mostly due to the assumption in Eq. (9). Such errors only occur in the temperature cases lower than 220 °C as shown in Figure 4(b). Mechanical properties of concrete do not degrade in such temperature level. Therefore, the errors do not affect computations of residual strengths.

Table 1 Variables of the maximum temperature for HEC and LEC

Variable		High energy case	Low energy case
$T^n_{0,CL}$	(°C)	$T^n_0 + \Delta T^n_{CL,\max}$	$100 + \Delta T^n_{CL,\max}$
$\Delta T^n_{CL,\max}$	(°C)	(2*b*-0.49)($T^n_0 - 521$) + 180	$0.53(100d_{LEC} - 18.56)^2 + 105.5$
α^n_{CL}		$\alpha^n + 1$	2.2
b_{CL}	(m)	b	d_{LEC}

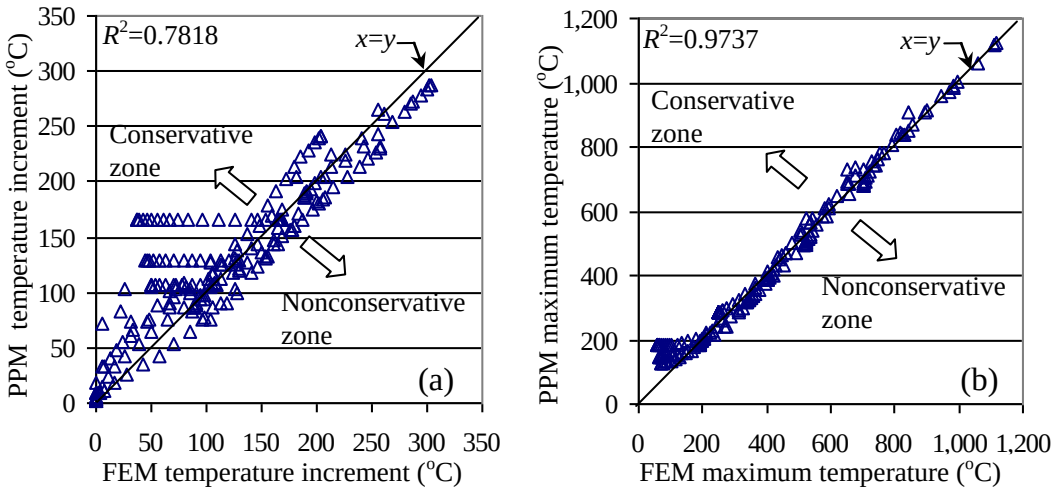

Figure 4 Overall comparisons of the proposed method (PPM) and the FEM results: (a) the temperature increment and (b) the maximum temperature

5. Conclusion

The maximum temperatures at each location of concrete sections exposed to a standard fire curve and cooling phases were investigated by a validated finite element (FE) model. One dimensional heat transfer analysis was a scope of this study. Investigated parameters were section thicknesses, fire durations and cooling durations. There are 90 FE models simulated. High energy cases (HECs) and Low energy cases (LECs) were considered as a type of temperature profiles in the sections. Temperatures of the non-fire exposed surface during the heating phase are significantly higher than the room temperature for the HECs, but about the room temperature for the LECs.

Comparing with at the end of the heating phase, increments of the maximum temperature for the HECs during the cooling phase monotonically increase with deeper depths due to heat energy in the sections is high enough to transfer throughout the sections. The temperature increments reach their maximum at the non-fire exposed surface. Magnitude of the maximum increment depends on the section thickness and magnitude of the temperature at the non-fire exposed surface at the end heating duration. For the LECs, the heat energy is not relatively high enough. The temperature increments are monotonically higher with deeper depths and reach their maximum at a certain depth and lower after that. The maximum increment was found at about the depth which having temperature of 100 ^{o}C at the end heating duration.

Based on an empirical study and an energy based method, equations to evaluate the maximum temperature increment and the maximum temperature at each deep after the cooling duration of 4 h were proposed. The overall maximum temperature profiles were represented as an exponent function. The profile exponent was also proposed. The temperature increment and the maximum temperature obtained from the proposed method agreed well with those of the FE results. The proposed method facilitates designing of residual structural strengths of an RC beam after fire.

6. References

[1] Bai LL, Wang ZQ. Residual bearing capacity of reinforced concrete member after exposure to high temperature. Advanced Materials Research 2011;368:577-81.

[2] Kodur VKR, Agrawal A. An approach for evaluating residual capacity of reinforced concrete beams exposed to fire. Engineering Structures 2016;110:293-306.

[3] Kodur VKR, Yu B, Dwaikat MMS. A simplified approach for predicting temperature in reinforced concrete members exposed to standard fire. Fire Safety Journal 2013;56:39-51.

[4] Wickstrom U. A very simple method for estimating temperature in fire exposed concrete structures. Fire Technology Technical Report SP-RAPP 1986: 46. London: Swedish National Testing Institute; 1986.

[5] Panedpojaman P. Spreadsheet Calculation of Energy Based Method to Predict Temperature in Concrete Slabs. International Review Civil Engineering 2012;3(5):403-411.

[6] Bratina S, Saje M, Planinc I. The effects of different strain contributions on the response of RC beams in fire. Engineering Structures 2007;29:418-430.

[7] Lim L, Wade C. Fire engineering research report 02/12 experimental fire tests of two-way concrete slabs. New Zealand: BRANZ Limited; 2012.

[8] Dwaikat MB and Kodur VKR. Response of restrained concrete beams under design fire exposure. Journal of Structural Engineering 2009;135(11):1408-1417.